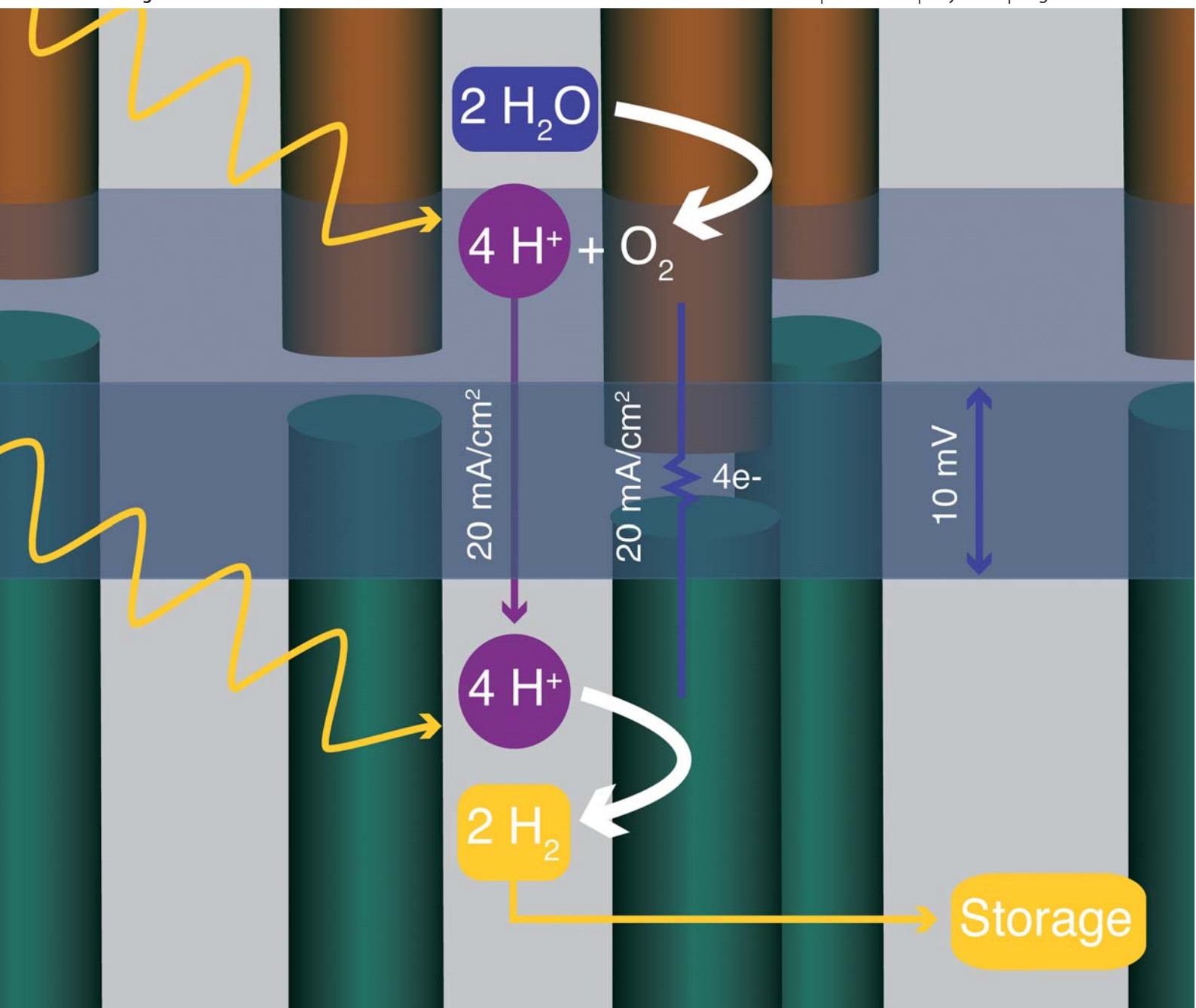


Energy & Environmental Science

www.rsc.org/ees

Volume 4 | Number 5 | May 2011 | Pages 1529–1928



ISSN 1754-5692

RSC Publishing

COVER ARTICLE

Lewis *et al.*

Designing electronic/ionic conducting membranes for artificial photosynthesis

COMMUNICATION

Chen *et al.*

Very low temperature membrane-free desalination by directional solvent extraction

Designing electronic/ionic conducting membranes for artificial photosynthesis†

Shaune L. McFarlane,^a Brittney A. Day,^a Kevin McEleney,^a Michael S. Freund^{*a} and Nathan S. Lewis^{*b}

Received 24th August 2010, Accepted 6th December 2010

DOI: 10.1039/c0ee00384k

We discuss the figures of merit for conducting membranes in artificial photosynthetic systems and describe an electronically and ionically conducting polymer composite with attractive performance characteristics.

One of the most interesting aspects of natural photosynthetic systems is the high-level of organization and exquisite juxtaposition of light harvesting, charge separating, charge relaying, redox catalyst systems achieved within a fluid-like membrane. In addition to acting as scaffolding for precisely coupled nanoscale modules, the membrane separates reductive and oxidative processes and efficiently manages electron and proton transport. Additional properties offered by nature's membrane-based systems include adequate physical and electrical contact between functional units, transparency to visible light, sufficient mechanical stability allowing for "free standing" membranes, and water insolubility.

Researchers from around the world are focused on developing artificial photosynthetic systems using various redox systems such as water or CO₂ as inputs and O₂ and reduced fuels as outputs.¹

However, research into the membranes required for these systems, as well as the figures of merit for such membranes, remains largely unexplored. Fig. 1 shows one possible design construct for an artificial photosynthesis system.² The system contains an assembly of micro- or nano-rod anodes (blue) and cathodes (red) embedded

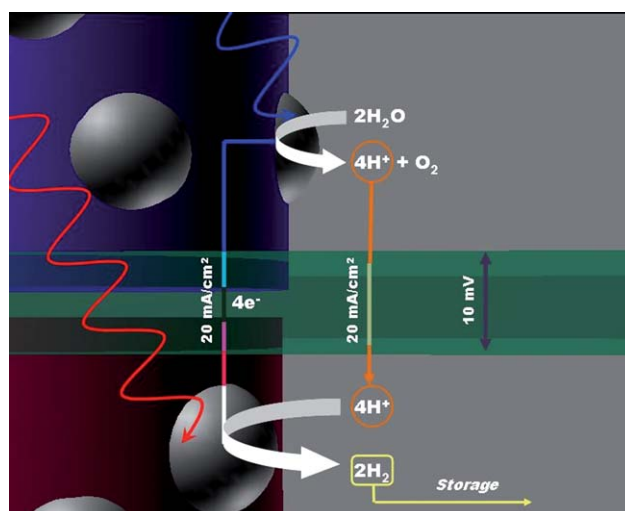


Fig. 1 Schematic of a technology for harnessing photons to convert water to O₂ and protons to H₂. The critical modules/processes in such a system are the photoanodes (blue), photocathodes (burgundy), membrane (green), catalyst (grey spheres), redox chemistry, ion and electron transport.

^aUniversity of Manitoba, Department of Chemistry, Winnipeg, Manitoba, Canada R3T 2N2. E-mail: michael_freund@umanitoba.ca; Fax: +1 204-475-7608; Tel: +1 204-474-8772

^bCalifornia Institute of Technology, Department of Chemistry, Pasadena, California, 91125, USA. E-mail: nslewis@caltech.edu; Fax: +1 626-395-8867; Tel: +1 626-395-8867

† Electronic supplementary information (ESI) available: Experimental details of membrane fabrication, membrane characterization (SEM, AFM, XPS, and AES), and detailed figure of merit calculations. See DOI: 10.1039/c0ee00384k

Broader context

To address future energy needs, while simultaneously stabilizing atmospheric CO₂ levels, scientists and engineers need to design and develop new materials and artificial photosynthetic device constructs that can effectively scale to meet society's vast and ever growing energy demands. A functional and effective artificial photosynthetic system will require the efficient production and separation of fuels that can be used as an on-demand source of energy. In contrast to fuel cells, such a system will require a membrane that conducts both ions associated with redox processes and electrons/holes associated with the absorption of light. Herein we discuss an approach to, and the figures of merit for, a membrane-based artificial photosynthetic design utilizing a composite material fashioned from state-of-the-art electronically and ionically conducting polymers. In particular, we demonstrate that while artificial photosynthetic systems that use these polymers as membrane materials have attractive electronic, ionic, physical, and optical properties, there are important tradeoffs, that in turn present opportunities for the design and synthesis of new materials to increase efficiencies.

within a proton- and electron-conducting membrane (green). Photosynthesis begins with the absorption of light and the generation of electron-hole pairs at the photoanodes and photocathodes. The holes and catalyst at the photoanodes oxidize the water to produce O_2 and protons, whereas the excited-state electrons and catalyst at the photocathodes reduce the protons to hydrogen.

In addition to transporting charge carriers and ions with minimal resistance, the membrane must be water insoluble, mechanically stable, optically transparent, homogeneous on the nanoscale, adherent to a wide range of semiconductors, electronically tuneable, impermeable to gases, and stable in the presence of redox intermediates and various pH conditions.

There is currently no single material capable of capturing the entire parameter space (*i.e.*, the 10 figures-of-merit listed above) for membrane-based artificial photosynthetic systems. The approach presented herein involves the development of conducting polymer composites with enhanced ionic conductivity. The rationale for using conducting polymers is that it is possible to tune the light absorbing properties³ as well as the charge carrier energy⁴ and Fermi level.⁵ This tunability is critical for creating effective junctions to arrays of photoelectrodes, and provides significant versatility for optimizing the overall properties of membranes for specific photosynthetic systems.

In this study, composite membranes were fabricated from the best two polymer candidates in terms of high optical transmission as well as high electron and proton conductivity. The materials investigated were electronically conducting poly(3,4-ethylenedioxythiophene)-poly(styrene sulfonate) (PEDOT-PSS) and ionically conducting perfluorinated ionomer, Nafion. PEDOT-PSS is a “work horse” polymer in the polymer electronics field because of its processability in the form of aqueous dispersions and its ability to form highly conductive, homogeneous, chemically stable and transparent films.⁶ Nafion has been used in polymer electrolyte membrane fuel cells (PEM-FC) since the 1970’s because of its high mechanical stability, high thermal and chemical stability, high proton conductivity, low hydrogen and oxygen permeability, and water insolubility.⁷ Both materials are commercially available as aqueous dispersions and can be processed into films that have excellent properties. The mutually similar anionic properties of PSS and Nafion are expected to facilitate formation of well-behaved, stable, homogeneous composites that are capable of addressing a number of the requirements of artificial photosynthetic membranes.

There is very little literature describing the fabrication of PEDOT/Nafion composites. For the most part, reports consist of attempts to either coat PEDOT onto existing Nafion membranes,⁸ or homogeneously disperse PEDOT into Nafion channels by chemically polymerizing EDOT within the pores of existing Nafion membranes.⁹ However, Wang and Olbricht recently prepared dense, smooth, and nearly uniform distributions of PEDOT and Nafion polymers in a PEDOT/Nafion composite by galvanostatic growth of PEDOT in the presence of commercially available alcoholic solutions of Nafion ionomer.¹⁰ The development of a method for simple mass production and greater compositional control is nevertheless required.

Composite membranes that contained varying weight percent of PEDOT-PSS were prepared by mixing commercially available aqueous dispersions of PEDOT-PSS and Nafion. The dispersions were indefinitely stable (>1 month) and showed no visible evidence of aggregation or flocculation. After drop-casting dispersions onto glass substrates, the films were allowed to dry overnight in ambient before thermal annealing for 90 min under vacuum at 110 °C. The resulting

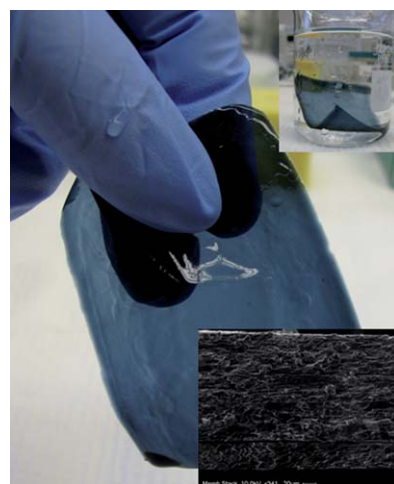


Fig. 2 Optical image of a free-standing membrane held in ambient and immersed in distilled water alongside an SEM micrograph containing a stack of six membranes.

freestanding, water insoluble, semi-transparent, and mechanically robust membranes were released from the glass by soaking in distilled water (Fig. 2).

Thermally annealed membranes were of sufficient mechanical strength that they could be repeatedly removed from the solution without any evidence of disintegration (>1 month), and could be rolled up, or lightly pulled repeatedly without ripping. In addition, membranes that contained up to 44% PEDOT-PSS had sufficient strength to be removed from solution and layered into a membrane stack (see ESI 2†). However, such membranes became increasingly brittle with increasing quantities of PEDOT-PSS. Fig. 2 shows a representative cross-section of a stack of ~40 μm thick composite membranes showing that the films were homogeneous, crack, and pinhole free on the micron scale when examined in cross-section with SEM (see AFM image in ESI 3† providing further support for crack and pinhole free composites). Additionally, XPS, Auger electron spectroscopy (AES) and AFM imaging of the composite membranes demonstrated that heterogeneity was significantly smaller than the 1–2 μm diameter rods that may be used in such a system (see ESI 3†). No significant evidence of chemical localization was observed by XPS or AES. XPS resolved the aromatic carbons of PEDOT-PSS from the fluorinated carbons of Nafion, however, composite XPS images revealed a homogeneous distribution of both types of carbon, as well as fluorine, across the sample (see ESI 4†). AES imaging revealed a similar level of homogeneity of the carbon and fluorine signal (see ESI 4†).

The flux of charge that an artificial photosynthetic membrane will be required to manage, and consequently the maximum resistance to charge-carrier flux that such a membrane can exhibit, is governed by the solar photon flux. Given a solar photon flux integrated over a region of interest to natural and artificial systems (400–700 nm) of $4.0 \text{ mmol s}^{-1} \text{ m}^{-2}$,¹¹ the corresponding current density passing through the membrane will be 20 mA cm^{-2} , assuming that one charge carrier traverses the membrane for every two incident photons absorbed by the photoelectrodes. In an ideal system no losses in voltage (1.23 eV thermodynamic driving force for splitting water)¹² would be present, however, if losses below 1% are deemed acceptable, then there should be no more than 10 mV iR loss for moving charges

through the membrane. At a current density of 20 mA cm^{-2} , the resistance of the membrane to moving charge carriers (electrons or holes) and ions should therefore not exceed $0.5 \Omega \text{ cm}^2$. Given a membrane area of 1 cm^2 , the conductivity, σ , in S cm^{-1} follows the relation $\sigma = 2L$, where L = membrane thickness in cm (see calculations in ESI†). This corresponds to 0.2 mS cm^{-1} per micron of membrane thickness, and thus implies a minimum required conductivity of 8 mS cm^{-1} for a membrane that is $40 \mu\text{m}$ thick. The ionic conductivity of conducting polymers is typically orders of magnitude lower than their electronic conductivity, so it is important to find a composition that optimizes both properties while simultaneously minimizing light absorption, since both iR losses and light absorption by the membrane will result in efficiency losses.

Electronic and ionic conductivities were determined as a function of the weight percent of PEDOT–PSS in the PEDOT–PSS/Nafion composites using a 4-point probe and a 4-electrode ionic conductivity cell,¹³ respectively (see calculations in ESI and ESI 5† for a picture of the 4-electrode ionic conductivity cell). As seen in Fig. 3, the composites exhibited pseudo-percolation behaviour with a threshold near 12% PEDOT–PSS. Composite films that were prepared by mixing alcohol solutions of Nafion ionomer and aqueous PEDOT–PSS exhibited pseudo-percolation thresholds near 9%, suggesting that changes to the solvent conditions would aid in lowering the quantity of conducting polymer required in the composites (see ESI 6†). However, these other composite membranes were not fully explored due to rapid flocculation (*i.e.*, flocculation was observed in $\sim 5 \text{ min}$). Composites prepared from aqueous Nafion that contained as little as 12% PEDOT–PSS exhibited electronic conductivities of $\sim 7.4 \text{ mS cm}^{-1}$, suggesting that $40 \mu\text{m}$ thick films of this material would be adequate for an artificial photosynthetic system. In contrast to the electronic conductivities, the ionic conductivities exhibited a more gradual transition from that of pure Nafion ($73 \pm 6 \text{ mS cm}^{-1}$) to that of a 12% PEDOT–PSS composite ($103 \pm 4 \text{ mS cm}^{-1}$) (Fig. 3). A decrease in ionic conductivity was expected after incorporating PEDOT–PSS,¹⁴ however, the ionic conductivity determined using 4-electrode ionic conductivity suggested otherwise. It is known that the conductivity of Nafion membranes increases with increasing membrane thickness ($\sim 0.7 \text{ mS cm}^{-1} \mu\text{m}^{-1}$ from 40 to $80 \mu\text{m}$),¹³

however, the increase in ionic conductivity of a 12% PEDOT–PSS/Nafion composite was $\sim 3.8 \text{ mS cm}^{-1} \mu\text{m}^{-1}$ (see ESI 7†). For drop cast Nafion membranes, results similar to Slade *et al.*¹³ were obtained ($\sim 0.6 \text{ mS cm}^{-1} \mu\text{m}^{-1}$ from 32 to $89 \mu\text{m}$), suggesting that additional factor(s) above film thickness is/are influencing the ionic conductivity of PEDOT–PSS/Nafion composites. While the ionic conductivity of PEDOT–PSS reported using electrochemical impedance¹⁴ is lower than those reported for Nafion membranes, the processing conditions used in fabricating the PEDOT–PSS films in that case were drastically different (*i.e.*, a load of 180 kg cm^{-2} for 90 s at 125°C). Under the conditions described herein a different trend is observed, suggesting that processing conditions impact conductivity and likely the morphology of the composite. Work is currently underway exploring this; however, at these loadings the trends are not significant and will likely not dramatically impact the performance in artificial photosynthetic systems.

In this system, PEDOT–PSS is fully oxidized and is in its most conductive state, suggesting that the conductivity of the composite cannot be increased nor can the weight percent of PEDOT–PSS be decreased by altering the composition. However, it is well known that morphological changes, effected in PEDOT–PSS films by various processing steps, can dramatically affect the electronic conductivity, with values as high as 900 S cm^{-1} having been reported.¹⁵ In addition to the opportunity for tuning the conductivity and percolation behaviour of PEDOT–PSS/Nafion composites, the smaller amounts of conducting polymer that may be required will result in membranes with lower light absorption. In addition, one can envision other electronically/ionically conducting materials, including composites composed of high-aspect-ratio materials (*i.e.*, carbon-nanotube/Nafion composites)¹⁶ or composites prepared with conducting polymer/carbon-nanotube dispersions¹⁷ and Nafion, with the potential to lower optical absorption losses. Indeed, the reduced percolation threshold observed for membranes created from alcohol dispersions may be due to the formation of high-aspect-ratio structures, as a result of partial flocculation during drying.

There will be a trade-off between the weight percent of PEDOT–PSS, and the thickness, conductivity, and absorbance of the membrane. Because the membrane absorbance changes as a function

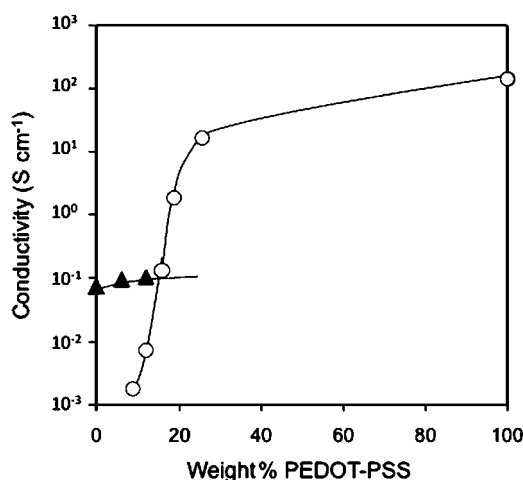


Fig. 3 Conductivity (○—electronic and ▲—ionic) of PEDOT–PSS/Nafion composites as a function of weight percent PEDOT–PSS in the composite.

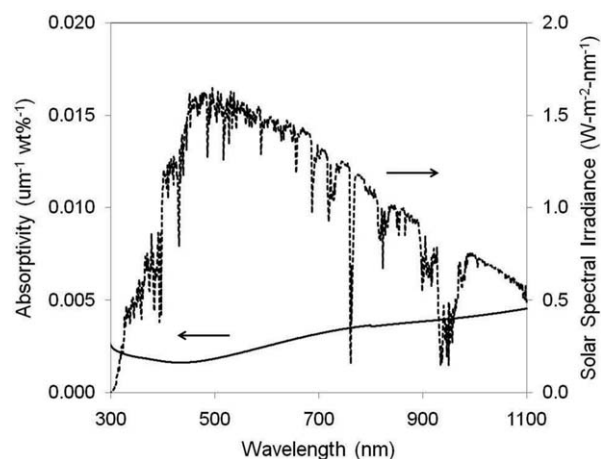


Fig. 4 UV-vis-NIR absorbance of a PEDOT–PSS/Nafion composite membrane normalized for film thickness and weight percent PEDOT–PSS plotted alongside the 2000 ASTM standard extraterrestrial solar spectral irradiance spectrum E4-490-0018 (dashed line).

of the weight percent PEDOT–PSS and as a function of thickness (see ESI 8†) the absorptivity of the membrane can be obtained by normalizing for thickness and weight percent PEDOT–PSS (Fig. 4). These results, in conjunction with the bulk conductivities in Fig. 3, allow determination of the figures-of-merit for a membrane with any composition/dimensions, and allow determination of the composition/dimensions that yield appropriate performance characteristics. For example, a 40 μm thick film that contains 12 wt% PEDOT–PSS would yield a conductivity of 7.4 mS cm^{-1} , similar to the 8 mS cm^{-1} limit discussed above. Assuming an average absorptivity of $0.002 \mu\text{m}^{-1} \text{ wt}\%^{-1}$ in the 400–700 nm region, a 12 wt% film that is 1 μm thick would have an absorbance of ~ 0.025 (i.e., 95% transmittance) (see calculations in ESI†). As discussed above, the development of electronic/ionic conducting composites that contain higher aspect ratio conducting materials should allow for reduced levels of electronically conducting polymers, and consequently decreased optical absorption. In addition, the development of new conducting polymers that have smaller band gaps, with “free carrier” absorption bands farther into the IR region will be important for the development of this field.

An additional factor that has the potential to impact the efficiency of artificial photosynthetic membrane-based systems is product crossover, related to transport of O_2 or H_2 , in this example. This issue is similar to that confronted by the fuel cell community, however in this case, the lower operating temperature and product solubility (e.g., solubility of O_2 and H_2 in water)¹⁹ will likely reduce the effects of crossover. In addition, crossover losses will be affected by the membrane thickness. For a 40 μm composite $\sim 5\%$ of the 20 mA cm^{-2} photogenerated current density will be lost due to product crossover (see ESI for calculations and ESI 1†). However, losses due to light absorption increase with film thickness, resulting in a trade-off between the effects of product crossover and light absorption (i.e., as membrane thickness increases, the performance of the photosynthetic system increases due to lower product crossover, but decreases due to lower light absorption). The optimum trade-off between product crossover and membrane thickness for a 12% PEDOT–PSS/Nafion composite is a membrane $\sim 7 \mu\text{m}$ thick. This would result in a combined loss of current due to light absorption and product crossover of $\sim 67\%$ (see ESI 1†).

Clearly, the trade-off between the optical and permeability properties of PEDOT–PSS/Nafion-based artificial photosynthetic membranes must be managed. This trade-off may be approached by (1) reducing the absorbance of the conducting polymer, (2) increasing the conductivity of the conducting polymer, (3) utilizing high-aspect-ratio conductors, (4) engineering the system to supply photons to both sides of the membrane, and/or (5) utilizing proton-conducting polymers with lower rates of product crossover. Work is currently under way in our laboratories exploring various approaches to each of these options.

Conclusions

Composites made from state-of-the-art electronically/ionically conducting polymers, namely PEDOT–PSS/Nafion, have attractive electronic, ionic, physical, and optical properties for artificial photosynthesis applications. However, trade-offs between weight percent PEDOT–PSS, thickness, conductivity, and absorbance result in significant optical and/or electrical losses due to the membrane. Given the large toolbox available for the synthesis, processability, and

tuning of polymer systems in general and ionic/electronic conducting polymers in particular, ionic/electronic conducting polymer composites can potentially make an important contribution to the design and fabrication of artificial photosynthetic systems. In particular, progress can be made by synthesizing new electronically conducting polymers with lower band gaps, by synthesizing new ionically conducting polymers with lower fuel crossover rates per unit membrane thickness, by incorporating polymers/materials with higher electronic conductivity and/or higher aspect ratios, or by the design/engineering of novel types of artificial photosynthesis devices. All of these approaches will be important to the future development of this field.

Acknowledgements

Financial support from the following is gratefully acknowledged: The Natural Sciences and Engineering Research Council (NSERC) of Canada, the Canada Foundation for Innovation (CFI), the Manitoba Research and Innovation Fund, the University of Manitoba, and made use of the Manitoba Materials and Surface Characterization Facility. This work was also supported by the NSF through a Center for Chemical Innovation, by the Stanford Global Trust and Energy Program, and by Toyota, and made use of the Molecular Materials Research Center of the Beckman Institute at Caltech, and the Kavli Nanoscience Institute at Caltech. This research was undertaken, in part, thanks to funding from the Canada Research Chairs Program. We thank Michael McDonald for the artwork in Fig. 1.

References

- 1 A. Listorti, J. Durrant and J. Barber, *Nat. Mater.*, 2009, **8**, 929–930.
- 2 N. S. Lewis and D. G. Nocera, *Proc. Natl. Acad. Sci. U. S. A.*, 2006, **103**, 15729–15735.
- 3 P. M. Beaujuge and J. R. Reynolds, *Chem. Rev.*, 2010, **110**, 268–320.
- 4 A. Facchetti, *Mater. Today*, 2007, **10**, 28–37.
- 5 P. A. Lane, P. J. Brewer, J. S. Huang, D. D. C. Bradley and J. C. deMello, *Phys. Rev. B: Condens. Matter Mater. Phys.*, 2006, **74**, 125320.
- 6 B. L. Groenendaal, F. Jonas, D. Freitag, H. Pielartzik and J. R. Reynolds, *Adv. Mater.*, 2000, **12**, 481–494.
- 7 C. J. Heitner-Wirguin, *J. Membr. Sci.*, 1996, **120**, 1–33.
- 8 S. J. Higgins, K. V. Lovell, R. M. G. Rajapakse and N. M. Walsby, *J. Mater. Chem.*, 2003, **13**, 2485–2489.
- 9 L. Li, J. F. Drillet, R. Dittmeyer and K. Juttner, *J. Solid State Electrochem.*, 2006, **10**, 708–713.
- 10 P. Wang and W. L. Olbricht, *Chem. Eng. J.*, 2010, **160**, 383–390.
- 11 O. Björkman, in *Physiological Plant Ecology I*, ed. O. L. Lang, P. S. Nobel, C. B. Osmond and H. Ziegler, Springer-Verlag, New York, 1981, vol. 12A, p. 59.
- 12 Z. G. Zou, J. H. Ye, K. Sayama and H. Arakawa, *Nature*, 2001, **414**, 625–627.
- 13 S. Slade, S. A. Campbell, T. R. Ralph and F. C. Walsh, *J. Electrochem. Soc.*, 2002, **149**, A1556–A1564.
- 14 M. Lefebvre, Z. G. Qi, D. Rana and P. G. Pickup, *Chem. Mater.*, 1999, **11**, 262–268.
- 15 Y. H. Ha, N. Nikolov, S. K. Pollack, J. Mastrangelo, B. D. Martin and R. Shashidhar, *Adv. Funct. Mater.*, 2004, **14**, 615–622.
- 16 J. Wang, M. Musameh and Y. H. Lin, *J. Am. Chem. Soc.*, 2003, **125**, 2408–2409.
- 17 M. C. Hermant, P. van der Schoot, B. Klumperman and C. E. Koning, *ACS Nano*, 2010, **4**, 2242–2248.
- 18 <http://rredc.nrel.gov/solar/spectra/am0/ASTM2000.html>.
- 19 D. R. Lide, *CRC Handbook of Chemistry and Physics*, CRC Press/Taylor and Francis, Boca Raton, FL, 90th edn.